Quantum kinetic derivation of the nonequilibrium Gross-Pitaevskii equation for nonresonant excitation of microcavity polaritons

H. Haug
Institut für Theoretische Physik, Goethe Universität Frankfurt, Max-von-Laue-Straße 1, D-60438 Frankfurt a.M., Germany

T. D. Doan and D. B. Tran Thoai
Ho Chi Minh City Institute of Physics, Vietnam Center for Natural Science and Technology, 1 Mac Dinh Chi, Ho Chi Minh City, Vietnam
(Received 29 October 2013; revised manuscript received 12 February 2014; published 2 April 2014)

The space and time dependent nonequilibrium Keldysh-Green functions are employed to derive the scattering rates between the condensed microcavity polaritons described by a Gross-Pitaevskii equation and an uncondensed higher lying exciton reservoir. Slowly varying center coordinates and rapidly varying relative coordinates are assumed. For particle-particle and particle-phonon interactions the scattering rates which provide gain to the condensate are calculated explicitly. These processes result in scattering rates which are quadratic and linear in the density of reservoir excitons, respectively. The resulting quantum Boltzmann equation for the reservoir is simplified by assuming local thermal equilibrium to rate equations for the exciton density and their temperature. Using the microscopically calculated (not phenomenologically chosen) transition amplitudes for CdTe microcavity polaritons we demonstrate that our model is able to describe the spontaneous pattern formation for a ring-shaped nonresonant excitation as seen in recent experiments

DOI: 10.1103/PhysRevB.89.155302 PACS number(s): 71.35.Lk, 78.47.jh, 78.20.Bh

I. INTRODUCTION

The Bose-Einstein condensation has been observed for trapped atomic gases cooled to extremely low temperatures [1–3]. In solid state physics transient bosonic condensations of magnons [4] and of exciton polaritons in microcavities (MCs) have been observed [5,6]. For the latter two examples a nonequilibrium description has to be used, because both magnons and the polaritons have finite lifetimes and have to be excited by laser pump pulses. The rich scenario of spatial structures such as vortices, solitons, and spontaneous pattern formation can be studied only in a real-space formulation, i.e., with a space and time dependent field rather than a single-mode description in momentum space. Assuming that the MC polaritons can be described as bosons, we start by considering the boson field operators $\psi(\vec{r},t)$ with the equal-time commutators

$$[\psi(\vec{r}_1,t),\psi^\dagger(\vec{r}_2,t)] = \delta(\vec{r}_1-\vec{r}_2). \tag{1}$$

Characteristic for a condensed boson system is the finite expectation value of the field operator

$$\langle\psi(X)\rangle = \Psi(X). \tag{2}$$

In the search to understand quantized vortices in quantum fluids such as He^4 and later condensed atomic gases Gross [7] and Pitaevskii [8] suggested independently using a simple Hartree approximation in order to derive the nonlinear Schrödinger equation

$$i\hbar\frac{\partial\Psi}{\partial t} = -\frac{\hbar^2\nabla^2}{2m_{\rm eff}}\Psi + g_0\Psi^\dagger\Psi\Psi, \tag{3}$$

where a point contact potential is used, which can be seen as the spatial integral over the real potential $g_0 = \int d^2r\, W(r)$. More generally g_0 is determined by the scattering length. An extension to spinor fields or wave functions describing in addition the two circular polarizations of the photons and the resonant excitons can be made straightforwardly [9]. Wouters and Carusotto [10] extended the Gross-Pitaevskii (GP) equation applied for MC polaritons to depict also nonequilibrium condensates by coupling the condensate to a reservoir of uncondensed particles which in turn is pumped by a laser. Seeing the success of the GP equation in condensed systems for understanding vortices, solitons, structure formation, and the Josephson oscillations between weakly coupled subsystems, we will also not attempt to go beyond the Hartree approximation for the condensate. The specific spectrum of microcavity (MC) exciton polaritons consists of a deep sharp part due to the cavity photon mode and a rather flat higher lying part of the spectrum due to the exciton mode as shown schematically in Fig. 1. The effective mass around the photon minimum is about a factor 10^{-4} smaller than the electron mass. As pointed out by Wouters and Savona [11] one can thus separate the system into a condensed fraction in the deep photon-like part and the uncondensed exciton reservoir. Scattering processes feed the condensed polaritons from the higher lying exciton reservoir which is replenished by laser pumping. A derivation of the nonequilibrium GP equation in terms of a density matrix formalism has already been given [11]. Here we formulate an alternative derivation in terms of nonequilibrium Green functions which we believe is particularly concise.

II. QUANTUM KINETIC DERIVATION OF THE NONEQUILIBRIUM GP EQUATION

In order to describe in the above introduced real-space formulation the scattering processes between the reservoir and the condensate, we use the nonequilibrium contour-time-ordered one-particle Green functions for the exciton-part of the system

$$G_1(X,X') = -i\langle T_c\psi(X)\psi^\dagger(X')\rangle, \tag{4}$$

where the time is defined on the Keldysh contour.

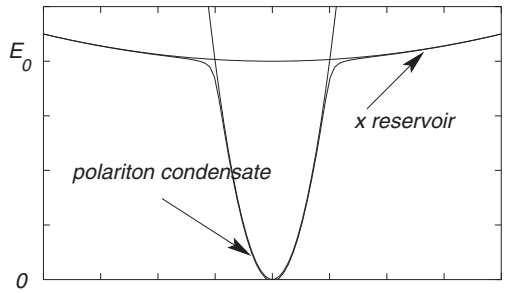

FIG. 1. Schematic plot of the lower branch polariton spectrum e_k. The two parabola are fits to the deep photon-like and the broad exciton-like parts of the polariton spectrum.

We largely make use of the techniques of Kadanoff-Baym [12] in order to derive the equations of motion for $\Psi(X)$ and for $G_1^<(X,X')$, i.e., the kinetic one-particle Green function for the uncondensed reservoir excitons. For contour-time-ordered functions—as we use them here—the derivations of the kinetic equations have been described in Ref. [13].

Note that here we employ the usual space, time, wave number, and frequency representation, while in former investigations of one of the authors (H.H.) of the semiconductor femtosecond spectroscopy [13] a separation into slow center coordinates and fast relative coordinates was not possible. There we started from the evolution equation for the equal-time kinetic function $G_k^<(t,t)$ and used—where necessary—a generalized Kadanoff-Baym relation to express approximately $G_k^<(t,t')$ in terms of retarded and advanced Green functions and $G_k^<(t,t)$. The used relation obeys causality. Because in the present problem the time variation of the exciting laser pulses is much slower—typically picoseconds instead of femtoseconds—one can make use of the separation in slow center and fast relative coordinates. A further important difference from our former work is that we treat here explicitly spatially inhomogeneous systems.

The analog to the Dyson equation for $\Psi(X)$ is given by

$$\Psi(X)=G_0(X,X')[\Sigma^n(X')\Psi(X')+\Sigma^a(X')\Psi^*(X')], \qquad (5)$$

where $G_0(X,X')$ is the free-particle propagator from X to X'; an integration over the repeated coordinates X' is assumed. The coherent nonlinear interaction gives rise to the normal one-point Hartree self-energy, which is $\Sigma^n(X)=\frac{1}{2}g_o\Psi(X)\Psi^*(X)$, while the corresponding anomalous self-energy is $\Sigma^a(X)=\frac{1}{2}g_o\Psi(X)\Psi(X)$ as shown in Fig. 2. Multiplying Eq. (5) from

FIG. 2. Normal and anormal first-order self-energy. The vertices represent the particle-particle interaction g_o. Particle conservation at the vertex requires two incoming and two outgoing particle lines. An incoming zigzag symbol represents a condensate line $\Psi(x)$.

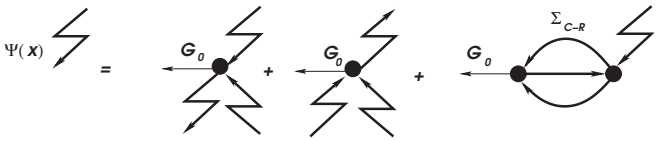

FIG. 3. Diagrammatic representation of the equation of motion for the order parameter wave function. The full lines are reservoir x Green's functions. The self-energy $\Sigma_{\frac{1}{2}}=\Sigma_{\mathrm{C-R}}$ describes the condensate-reservoir coupling.

the left by

$$G_0^{-1}(X,X')=\left(i\hbar\frac{\partial}{\partial t}+\frac{\hbar^2\nabla^2}{2m_c}-U(X)\right)\delta(X,X'),$$

we get the free Gross-Pitaevskii equation (3) for the cavity polaritons with an external potential $U(r,t)$:

$$\left(i\hbar\frac{\partial}{\partial t}+\frac{\hbar^2\nabla^2}{2m_c}-U(X)\right)\Psi(X)=g_0|\Psi(X)|^2\Psi(X). \qquad (6)$$

For MC polaritons the condensate has now to be coupled to the reservoir which we assume—as discussed above—to be noncondensed and to have the dispersion of the quantum well excitons with an effective mass $m_x \gg m_c$. The corresponding equation of motion for condensate wave function $\Psi(X)$ which we consider as the lowest Green function $G_{\frac{1}{2}}$ in the hierarchy of the n-particle Green functions is shown in Fig. 3 diagrammatically. The last diagram shows the coupling to the x reservoir. Note, in the last diagram one has to integrate over repeated arguments, i.e., over X' in $\Sigma_{\frac{1}{2}}(X,X')\Psi(X')$, which remains after the multiplication from the left-hand side with G_0^{-1}.

In the term

$$\Sigma_{\frac{1}{2}}(X,X')\Psi(X'), \qquad (7)$$

we introduce slowly varying center coordinates $\mathbf{R},T$ and the relative coordinates $\mathbf{r}=\mathbf{x_1}-\mathbf{x_2}, t=t_1-t_2$. The time t_2 has to be integrated over the Keldysh contour running from $-\infty$ to t_1 and back to $-\infty$. The relative time t runs thus 0 to ∞ and back to 0 which yields

$$\Sigma_{\frac{1}{2}}(X,X')\Psi(X') \simeq \int d^2r\int_0^\infty dt\left(\Sigma_{\frac{1}{2}}^>(\mathbf{R},T,\mathbf{r},t)-\Sigma_{\frac{1}{2}}^<(\mathbf{R},T,\mathbf{r},t)\right)\Psi(\mathbf{R},T). \qquad (8)$$

Note, by taking the condensate field only at the center coordinates we neglect possible nonlocalities and memory effects. Here the nonequilibrium self-energy is defined as, e.g., $\Sigma_{\frac{1}{2}}(X_1,X_2)=\Sigma_{\frac{1}{2}}^>(X_1,X_2)$ for $t_1>t_2$ on the Keldysh contour. The difference $\Sigma^>-\Sigma^<$ is the difference between the scattering rates in and out of the condensate; i.e., these terms determine the gain of the condensate due to the coupling to the reservoir. From the scattering diagram with 3 inner propagators in Fig. 3 we get, e.g., for the integrals over

r and t of the function $-\Sigma^{<}_{\frac{1}{2}}(\mathbf{R},T,\mathbf{r},t)$,

$$
\begin{aligned}
&-ia_3\int d^2r\int_0^\infty dt g_0^{\text{x-c},2}G^<(X,X')G^<(X,X')G^>(X',X)\\
&\quad=-ia_3\int d^2r\int_0^\infty dt g_0^{\text{x-c},2}(\mathbf{r})\\
&\qquad\times G^<(\mathbf{R},T,\mathbf{r},t)G^<(\mathbf{R},T,\mathbf{r},t)G^>(\mathbf{R},T,-\mathbf{r},-t). \qquad (9)
\end{aligned}
$$

In the evaluation of the self-energy $\Sigma_{\frac{1}{2}}$ we include a phase factor a_3 for the diagram containing 3 propagators. We will determine this phase factor so that the particle conservation between condensate and reservoir holds:

$$
\frac{d|\Psi(\mathbf{R},T)|^2}{dT}=-\frac{dN_x(\mathbf{R},T)}{dT}, \qquad (10)
$$

where $N_x(\mathbf{R},T)$ is the density of reservoir excitons. Next we insert Fourier transforms with respect to the rapidly varying relative coordinates (for shortness we omit the central coordinates)

$$
\begin{aligned}
&-ia_3\sum\int d^2r\int_0^\infty dt G^<(\mathbf{k_1},\omega_1)G^<(\mathbf{k_2},\omega_2)G^>(\mathbf{k_3},\omega_3)\\
&\quad\times g_0^{\text{x-c},2}e^{i((\mathbf{k_1}+\mathbf{k_2}-\mathbf{k_3})\cdot\mathbf{r}-(\omega_1+\omega_2-\omega_3)t)}\\
&\quad=-ia_3\sum\int_0^\infty dt G^<(\mathbf{k_1},\omega_1)G^<(\mathbf{k_2},\omega_2)G^>(\mathbf{k_1}+\mathbf{k_2},\omega_3)\\
&\qquad\times g_0^{\text{x-c},2}e^{-i(\omega_1+\omega_2-\omega_3)t}, \qquad (11)
\end{aligned}
$$

where $g_0^{\text{x-c}}$ is the matrix element for the scattering of a condensate polariton to a reservoir exciton. A dependence on the transferred momentum has been disregarded in the derivation, but can simply be inserted in the final result if necessary. Next we use the Kadanoff-Baym ansatz to introduce a distribution function $f(\mathbf{R},T,k)$ by writing the kinetic Green function

$$
\begin{aligned}
G^<(\mathbf{R},T,\mathbf{k},\omega)&=-iA(\mathbf{R},T,\mathbf{k},\omega)f(\mathbf{R},T,\mathbf{k}),\\
G^>(\mathbf{R},T,\mathbf{k},\omega)&=-iA(\mathbf{R},T,\mathbf{k},\omega)[1+f(\mathbf{R},T,\mathbf{k})].
\end{aligned} \qquad (12)
$$

Here $-iA(\mathbf{R},T,\mathbf{k},\omega)=G^r-G^a=G^>-G^<$ is the spectral function, while the distribution function depends only on R,T,k in the spirit of the Boltzmann kinetics. In this spectral function the collision broadening, e.g., can be integrated by solving the Dyson equation for the retarded Green function. A spectral function which contains collision broadening can be chosen in the form

$$
A(\mathbf{k},\omega)=\frac{2\gamma(N_x)}{(\omega-e_k)^2+\gamma^2(N_x)}, \qquad (13)
$$

where $\gamma(N_x)=\gamma_x(1+\frac{N_x}{N_s})$ with a phenomenologically introduced x-saturation density N_s. In the simpler quasiparticle approximation $A(\mathbf{k},\omega)=2\pi\delta(\omega-e_k)$ one gets from the time and frequency integrations over the product of the spectral functions

$$
\begin{aligned}
&a_3g_0^{\text{x-c},2}\lim_{\gamma\to0}\sum\int_0^\infty dt f_{k_1}f_{k_2}(1+f_{k_1+k_2})\\
&\quad\times e^{-i(\omega_1+\omega_2-\omega_3)t-\gamma t}\delta(\omega_1-e_{k_1})\delta(\omega_2-e_{k_2})\delta(\omega_3-e_{k_1+k_2})\\
&\quad=a_3g_0^{\text{x-c},2}\sum\lim_{\gamma\to0}\frac{f_{k_1}f_{k_2}(1+f_{k_1+k_2})}{i(e_{k_1}+e_{k_2}-e_{k_1+k_2})+\gamma}\\
&\quad=-ia_3g_0^{\text{x-c},2}\lim_{\gamma\to0}\sum\left(\frac{\gamma}{(e_{k_1}+e_{k_2}-e_{k_1+k_2})^2+\gamma^2}\right.\\
&\left.-i\frac{e_{k_1}+e_{k_2}-e_{k_1+k_2}}{(e_{k_1}+e_{k_2}-e_{k_1+k_2})^2+\gamma^2}\right)f_{k_1}f_{k_2}(1+f_{k_1+k_2})\\
&\quad=a_3g_0^{\text{x-c},2}\sum\left(\pi\delta(e_{k_1}+e_{k_2}-e_{k_1+k_2})\right.\\
&\left.-i\text{P}\frac{1}{e_{k_1}+e_{k_2}-e_{k_1+k_2}}\right)f_{k_1}f_{k_2}(1+f_{k_1+k_2}); \qquad (14)
\end{aligned}
$$

i.e., one gets next to the scattering rate also the dispersive contribution due to these transitions. The self-energy term $\Sigma^{>}_{\frac{1}{2}}$ yields a similar scattering rate from the condensate to the reservoir with the occupation function $(1+f_{k_1})(1+f_{k_2})f_{k_1+k_2}$. Putting all terms together one finds finally the contribution to the GP equation by the choice of the phase factor $a_3=i$,

$$
\Sigma^{\text{x-c}}_{\frac{1}{2},\text{p-p}}(\mathbf{R},T)=\frac{i\hbar}{2}R^{\text{x-c}}_{\text{p-p}}\Psi(\mathbf{R},T), \qquad (15)
$$

which we expressed in terms of a complex scattering amplitude $R^{\text{x-c}}_{\text{p-p}}$ for particle-particle scattering between the reservoir and the condensate. This scattering amplitude has the dimension of a frequency.

If one of the particles is scattered up into an unoccupied state with $f_{k+k'}\simeq0$, while the other one is scattered down into the condensate, excitonic gain results, i.e., gain without inversion,

$$
f_kf'_k(1+f_{k+k'})-(1+f_k)(1+f_{k'})f_{k+k'}\simeq f_kf_{k'}. \qquad (16)
$$

We use the short-hand notation $f_{\mathbf{k}}=f(\mathbf{R},T,\mathbf{k})$. The minimum of the effective x spectrum is at E_0 (see Fig. 1). Thus $e_{\mathbf{k}}=\epsilon_{\mathbf{k}}+E_0$, where $\epsilon_k=\hbar^2k^2/(2m_x)$. This replacement changes the energy conserving delta function in the scattering integral into $\delta(\epsilon_{\mathbf{k}}+\epsilon_{\mathbf{k}'}+E_0-\epsilon_{\mathbf{k}+\mathbf{k}'})$, where E_0 as shown in Fig. 1 is the minimum energy of the parabola fitted to the exciton reservoir. All levels shift to the blue with increasing density but the shifts are approximately the same for the condensate and the reservoir and thus drop out of the energy differences. The resulting scattering amplitude for p-p scattering is the scattering rate (in the final result $\hbar$ is restored where needed, because it was put equal to 1 in the derivation)

$$
\text{Re}R^{\text{x-c}}_{\text{p-p}}=\frac{2\pi}{\hbar}\sum_{\mathbf{k},\mathbf{k}'}g_0^{\text{x-c},2}f_{\mathbf{k}'}f_{\mathbf{k}}\delta(\epsilon_{\mathbf{k}}+\epsilon_{\mathbf{k}'}+E_0-\epsilon_{\mathbf{k}+\mathbf{k}'}), \qquad (17)
$$

and the frequency shift

$$
\text{Im}R^{\text{x-c}}_{\text{p-p}}=-\frac{2}{\hbar}\text{P}\sum_{\mathbf{k},\mathbf{k}'}g_0^{\text{x-c},2}\frac{f_{\mathbf{k}'}f_{\mathbf{k}}}{\epsilon_{\mathbf{k}}+\epsilon_{\mathbf{k}'}+E_0-\epsilon_{\mathbf{k}+\mathbf{k}'}}. \qquad (18)
$$

This dispersive shift contained in (18) will add to the blueshift contained in the nonlinear self-interaction term. The gain (17) and the dispersive shift (18) agree with the corresponding results Eqs. (15) and (16) of Ref. [14] derived by an equation of motion technique combined with an adiabatic elimination in a single-mode theory for the line shape calculation of a spatially homogeneous condensate. The detailed evaluation of the scattering amplitude will be postponed until we have derived also the kinetic equation for the reservoir excitons in which the scattering rate $\text{Re}R^{\text{x-c}}_{\text{p-p}}$ will appear again. Naturally,

there is also a radiative loss term in the form $-\gamma_c\Psi$ which can simply be derived by a coupling to a vacuum photon bath. With the p-p scattering amplitude the resulting nonequilibrium GP equation has the form

$$\left(i\hbar\frac{\partial}{\partial T}+\frac{\hbar^2\nabla^2}{2m_c}-U(\mathbf{R},T)\right)\Psi(\mathbf{R},T) = g_0|\Psi(\mathbf{R},T)|^2\Psi(\mathbf{R},T)+\frac{i\hbar}{2}\left(R_{\text{p-p}}^{\text{x-c}}-2\gamma_c\right)\Psi(\mathbf{R},T), \quad (19)$$

which has exactly the form postulated by Wouters and Carusotto [10]; however the x-c scattering amplitude was assumed to be linear in the x reservoir density. This equation with its microscopically derived scattering amplitudes will be discussed in Sec. V, after we have also included the contributions of phonon-assisted transitions between the x reservoir and the condensate.

III. KINETIC EQUATION FOR THE RESERVOIR EXCITONS

Next we calculate the kinetic equation for the reservoir of uncondensed excitons. The propagator $G^<(X,X') = -i\langle\psi^\dagger(X')\psi(X)\rangle$ is obtained from the general nonequilibrium Green function, if the contour time t_c is less than t_c'. $G^<$ governs the kinetics of the excitons in the reservoir.

The second-order p-p scattering self-energy between the reservoir and the condensate is shown in Fig. 4 and is given by

$$\Sigma^{\text{c-x}}(X,X') = ig_0^{\text{x-c},2} \times\Psi^*(X)G_1(X,X')G_1(X',X)\Psi(X'). \quad (20)$$

We briefly describe the quantum kinetic derivation of the kinetic equation for the uncondensed reservoir excitons in the form of a generalized Boltzmann equation [13]. The starting point is the left and right hand Dyson equation for the contour-time-ordered one-particle Green function G_1:

$$G_1 = G_0 + G_0\Sigma^{c,x}G_1, \quad G_1 = G_0 + G_1\Sigma^{\text{c-x}}G_0, \quad (21)$$

where the self-energy is given by (20). Pumping will be included later. The kinetics is governed by $G^<(X,X') = -i\langle\psi^\dagger(X')\psi(X)\rangle$. By straightforward calculations [13] one gets from these two equations the Kadanoff-Baym equation

$$\left[G_0^{-1},G^<\right] = \{\Sigma^>,G^<\} - \{\Sigma^<,G^>\}, \quad (22)$$

where [,] and { , } are the commutator and anticommutator, respectively. We used relations like $G^r = G^> - G^<$ and $G^a = G^< - G^>$. Because $G^< \propto f$ and $G^> \propto (1+f)$, the scattering rates on the right-hand side in which a $G^<$ occurs are scattering rates out of the considered state, while those with a final state population factor $G^>$ are scattering rates into this state. Next we introduce center and relative coordinates $\mathbf{R} = \frac{1}{2}(\mathbf{x}_1+\mathbf{x}_2)$, $T = \frac{1}{2}(t_1-t_2)$ and $\mathbf{r} = \mathbf{x}_1 - \mathbf{r}_2$, $t = t_1 - t_2$ and take Fourier transforms with respect to $\mathbf{r},t$ which yields the spectral variables $\mathbf{k},\omega$. After this transformation the two-point functions become $B(X,X') \to B(\mathbf{R},T,\mathbf{k},\omega)$. Commutators and anticommutators as they appear in (22) take in the lowest gradient approximation the forms

$$[B,C]_{\mathbf{R},T,\mathbf{k},\omega} = -i\left(\frac{\partial B}{\partial T}\frac{\partial C}{\partial\omega}-\frac{\partial B}{\partial\omega}\frac{\partial C}{\partial T}-\frac{\partial B}{\partial\mathbf{R}}\cdot\frac{\partial C}{\partial\mathbf{k}}+\frac{\partial B}{\partial\mathbf{k}}\cdot\frac{\partial C}{\partial\mathbf{R}}\right), \quad (23)$$

$$\{B,C\}_{\mathbf{R},T,\mathbf{k},\omega} = 2B(\mathbf{R},T,\mathbf{k},\omega)C(\mathbf{R},T,\mathbf{k},\omega). \quad (24)$$

Inserting $G_0^{-1}(\mathbf{R},T,\mathbf{k},\omega) = \omega - \frac{\hbar k^2}{2m_x} - U(\mathbf{R},T)/\hbar$ and integrating over ω the Kadanoff-Baym equation becomes

$$\left(\frac{\partial f}{\partial T}+\frac{\hbar\mathbf{k}}{m_x}\cdot\frac{\partial f}{\partial\mathbf{R}}-\frac{\partial U}{\partial\mathbf{R}}\cdot\frac{\partial f}{\partial\hbar\mathbf{k}}\right) = P(\mathbf{R},T,\mathbf{k}) - 2\gamma_x f_k + \text{Re}\, r_k^{\text{x-c}}|\Psi(\mathbf{R},T)|^2 + r_k^{\text{x-x}} + r_k^{\text{x-phon}}. \quad (25)$$

This quantum Boltzmann equation describes the spatial-temporal variation of the x distribution $f_{\mathbf{k}}(\mathbf{R},T)$ in the presents of an x-c coupling. The radiative loss term $-2\gamma_x f_{\mathbf{k}}$ in the reservoir equation and a corresponding loss term in the order parameter equation $-\gamma_c\Psi$ have been included without explicit derivation. These terms can easily be derived quantum kinetically by coupling the considered particles to a photon vacuum bath. A similar derivation can be given for the incoherent pump process which has also be included with the pump rate $P(\mathbf{R},T,\mathbf{k})$ in the reservoir equation. The last two terms in (25) have been added without derivation to remind the reader that there is naturally also inter-reservoir scattering by x-x and x-phonon interactions, but these processes do not change the number of excitons in the reservoir. The inter-reservoir x-x scattering rate, e.g., is given by

$$r_k^{\text{x-x}} = -\frac{2\pi}{\hbar}\sum g_q^{\text{x-x},2}\delta(e_k+e_{k'}-e_{k+q}-e_{k'-q}) \times\{f_kf_{k'}(1+f_{k+q})(1+f_{k'-q}) - (1+f_k)(1+f_{k'})f_{k+q}f_{k'-q}\}, \quad (26)$$

where $g_q^{\text{x-x}}$ is the x-x scattering matrix element. The x-phonon interaction $r_k^{\text{x-ph}}$ is considered in the Appendix in connection with the heat transfer from the x bath to the lattice.

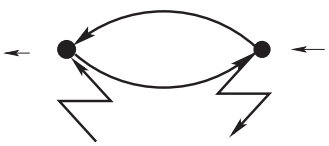

FIG. 4. Second-order scattering self-energy $\Sigma_{\text{p-p}}^{\text{x-c}}$ for G_1.

A. Reservoir-condensate scattering rate

The right-hand side of the general kinetic equation (25) becomes from (20)–(22) in the quasiparticle approximation

$A = 2\pi\delta(\omega - e_k)$ again after an integration over ω

$$-\mathrm{Re}\, r_k^{\text{x-c}}\, |\Psi(\mathbf{R},T)|^2 = -\frac{2\pi}{\hbar}\sum_{\mathbf{k}'} g_0^{\text{c-x},2}|\Psi(\mathbf{R},T)|^2\delta(e_{\mathbf{k}} + e_{\mathbf{k}'} - e_{\mathbf{k}+\mathbf{k}'}) \times [f_{\mathbf{k}'} f_{\mathbf{k}}(1 + f_{\mathbf{k}+\mathbf{k}'}) - (1 + f_{\mathbf{k}'})(1 + f_{\mathbf{k}}) f_{\mathbf{k}+\mathbf{k}'}]. \quad (27)$$

We estimate the x-c scattering matrix element by its long-wavelength limit putting all x-Hopfield coefficients in the reservoir range equal to 1:

$$g_0^{\text{c-x}} \simeq \frac{6E_R a_0^2}{F} u^x_{k=0} = \frac{3E_R a_0^2}{F}. \quad (28)$$

E_R and a_0 are the 2D x Rydberg and Bohr radius, respectively. The x-Hopfield coefficient at $k = 0$ is for the case of zero detuning $u^x_{k=0} = \frac{1}{2}$. If we use the same arguments to determine the p-p interaction in the condensate we get with three more exciton Hopfield coefficients at $k = 0$ the formula

$$g_0 = \frac{3E_R a_0^2}{8F}. \quad (29)$$

Compared to the condensate-exciton reservoir scattering matrix element $g_0^{\text{c-x}}$ the blueshift matrix element g_0 is eight times smaller. In the numerical evaluation of our theory for structure formation we will use the relatively small value (29). Because of the neglected momentum transfer in the c-x matrix element, g_0 may be somewhat larger than $g^{\text{c-x}}/8$.

Note that the particle-particle scattering rate (27) is bilinear in the distribution function f; the back-scattering term can be neglected because for the higher lying final state $f_{\mathbf{k}+\mathbf{k}'} \simeq 0$ as already discussed for the GP equation above.

A comparison with the GP equation shows that $1/2$ of the loss rate in the Boltzmann equation summed over k enters as a gain into the GP equation, as required by particle conservation.

B. Simplifications for a reservoir in local equilibrium

In general situations with spatiotemporal variations of the order parameter and the x-distribution function $f_{\mathbf{k}}(\mathbf{R},T)$ the numerical solution would be extremely extensive. Because the main physical interest concerns the spatial and temporal variation of the condensate, the treatment of the reservoir should be kept as simple as possible. Therefore Wouters and others [10,11,15] used only a simple rate equation for the total x density in the reservoir. We go one step further by simplifying the above derived quantum Boltzmann equation by assuming a local (by no means global) thermal equilibrium in which the inter-reservoir scattering rates (26) drop out due to detailed balance. The local equilibrium distribution can in general be expressed in terms of collision invariants. For the dominate x-x scattering alone, the conserved quantities are the particle number, the momentum, and the energy. The corresponding local equilibrium Bose distribution is

$$f^0_{\mathbf{k}}(\mathbf{R},T) = \frac{1}{e^{\beta_x(\mathbf{R},T)(e_k - \hbar\mathbf{k}\cdot\mathbf{u}_x(\mathbf{R},T) - \mu_x(\mathbf{R},T))} - 1}. \quad (30)$$

Here $\beta_x(\mathbf{R},T), \mathbf{u}_x(\mathbf{R},T), \mu_x(\mathbf{R},T)$ are the inverse temperature, drift velocity, and chemical potential of the x reservoir, respectively. These quantities are determined by the corresponding hydrodynamic equations. Because one does not expect condensation in the reservoir, one can simplify the general Bose distribution (30) by a Boltzmann distribution for a nondegenerate Bose gas. Summing the Boltzmann distribution over all k values, $\frac{1}{F}\sum_{\mathbf{k}} f_{\mathbf{k}} = N_x(\mathbf{R},T)$, where F is the cross section of the MC, one gets the total 2D x density N_x. The thermalized nondegenerate 2D x distribution is

$$f_{\mathbf{k}} = N_x(\mathbf{R},T)\left(\frac{2\pi\hbar^2\beta_x(\mathbf{R},T)}{m_x}\right) e^{-\beta_x(\mathbf{R},T)\epsilon_k}, \quad (31)$$

where we used the fact that in a 2D system the chemical potential can be expressed analytically in terms of the total density [16]. We also dropped the drift term, because a drift of the reservoir would be strongly damped by the coupling of the x-phonon coupling. However, if with a special excitation a strong drift is induced, one can include this effect also by generalizing the rate equation to a continuity equation with a drift term in the form $\nabla\cdot\mathbf{j}(\mathbf{R},T)$, with the current density $\mathbf{j}$. The rate equation which follows from the summed quantum Boltzmann equation (25) is

$$\frac{\partial N_x}{\partial T} = P(\mathbf{R},T) - \mathrm{Re}R^{\text{x-c}}_{\text{p-p}}(\mathbf{R},T)|\Psi(\mathbf{R},T)|^2 - 2\gamma_x N_x. \quad (32)$$

The coupling rate of the excitons to the condensate results from (27) with (31):

$$\mathrm{Re}R^{\text{x-c}}_{\text{p-p}} \simeq \pi N_x^2 g_0^{\text{c-x},2} F^2 \frac{\beta_x}{\hbar} e^{-\beta E_0}. \quad (33)$$

The sum of the two momenta $\mathbf{k} + \mathbf{k}'$ has to be large enough to reach an unpopulated state and to scatter one particle sufficiently down into the condensate. β_x^{-1} is a measure of the energy width over which the excitons contribute to the transitions into the condensate. Similarly one can evaluate the principal value integral of the dispersive shift (18). Integrating first over the angle between $\vec{k},\vec{k}'$ one gets for a parameter $(E_0 - \mu_c)/\hbar^2 kk'/m \geqslant 1$ the value of $\pi/2$ for this angle integral. The integral over k' yields an error function of the argument $1/k$. The final integral over k from the error function times a Gaussian yields the remarkably simple final result

$$\mathrm{Im}R^{\text{x-c}}_{\text{p-p}} = -\frac{\pi^2 g_0^{\text{c-x},2} F^2 N_x^2 \beta_x}{2\hbar}, \quad (34)$$

provided the parameter $\beta_x E_0 \gg 1$ which is well fulfilled. Note again that the transition rate and the corresponding dispersive shift are quadratic in the reservoir x density N_x as it should be for a p-p scattering rate. The dispersive shift combines with the blueshift term in the nonequilibrium GP equation (20) to an "extended blueshift"

$$\frac{g_0 N_0(\mathbf{R},T)}{\hbar} + \frac{\pi^2 g_0^{\text{c-x},2} F^2 N_x(\mathbf{R},T)^2 \beta_x}{2\hbar}. \quad (35)$$

Thus there is not only a blueshift proportional to the condensate density N_0, but due to the coupling to the reservoir also one which increases with the square of the x-reservoir density N_x. Such a quadratic shift has already been observed below the condensate threshold [17]. This sub-threshold region can be described by a stochastic extension of the nonequilibrium GP equation (see Sec. V).

Before we turn to the derivation of an equation for the local reservoir temperature, we want to discuss the limitations of our approach. The description of the pumped reservoir in terms of bosonic excitations, which are furthermore nondegenerate and in local equilibrium, may not hold directly during an intensive pump pulse, but may hold only somewhat after pump pulse, when an initial thermalization of the primarily excited electrons and holes has already taken place.

C. Derivation of a rate equation for the local x temperature

In local thermal equilibrium we may still have slowly varying exciton temperature $T_x(\mathbf{R},T) \geqslant T_b$ larger than the bath temperature T_b. Its equation of motion can be obtained by multiplying the Boltzmann equation with the x translational energy ϵ_k using the relation

$$N_x(\mathbf{R},T)k_BT_x(\mathbf{R},T) = \frac{1}{F}\sum_{\mathbf{k}} \epsilon_k f_k(\mathbf{R},T), \tag{36}$$

which in 2D is just the thermal x energy density. Assuming that we excite by wide-angle excitation excitons with a momentum k_p, one can write the pump rate as

$$\frac{1}{F}\sum_{\mathbf{k}} \epsilon_k P_k(\mathbf{R},T) = P(\mathbf{R},T)\epsilon_p, \tag{37}$$

with $\epsilon_p = \epsilon_{k_p}$. Similarly the radiative loss term can be written as $-2\gamma_x N_x k_B T_x$. As shown in the Appendix the coupling to the thermal acoustic phonons results in a cooling rate $N_x k_B(T_b - T_x)/\tau^{ac}$, where τ^{ac} is the x-phonon relaxation time (A6). This form can be obtained by making a relaxation time approximation to the inter-reservoir x-phonon scattering rates. The coupling to the condensate causes a loss rate of energy (assuming that the energy of the x scattered to higher energy is directly absorbed by the phonon bath)

$$\frac{1}{F}\sum_{\mathbf{k}} \epsilon_k r_k^{\text{x-c}} \simeq -N_x^2 g_0^2 |\Psi|^2. \tag{38}$$

The two rate equations for N_x and for $N_x k_B T_x$ yield the rate equation for the thermal energy per particle:

$$\frac{dk_BT_x}{dT} = \frac{P(\mathbf{R},T)}{N_x}\left(\epsilon_p - k_BT_x\right) + \frac{k_B(T_b - T_x)}{\tau^{ac}}. \tag{39}$$

The first term describes the energy rate generated by the pump pulse, which relaxes toward the bath thermal energy according to the second term. Thus this equation describes how the pumping deposits heat and how the x temperature relaxes from this hot spot towards the bath temperature. The additional equation (39) for the thermal x energy could perhaps replace the rate equation of "inactive excitons" which had to be used in order to describe the dynamics of spontaneous quantum vortices in accordance with the experiment [18]. More generally it has been found that such a second reservoir equation has to be used in situations with large deviations from thermal equilibrium [19], where the reservoir temperature will certainly be higher than the lattice temperature and will require its own equation of motion. Thus the heat flow from the hot spots to the cooler regions could replace the higher lying bath of "inactive excitons" in Ref. [18]. Both rate equations for $N_x(\mathbf{R},T)$ and $k_BT_x(\mathbf{R},T)$ can be completed by a corresponding diffusion term if necessary.

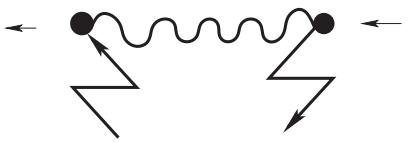

FIG. 5. Second-order x-phonon scattering self-energy $\Sigma^{\text{x-c}}_{\text{x-ph}}$. The phonon is shown by a wavy line; the vertex here describes the x-phonon interaction.

D. Evaluation of the particle-phonon scattering amplitude

Another scattering channel from the reservoir to condensate is the scattering by phonon emission. Longitudinal acoustic (a) and longitudinal optical (LO) phonons have energies (typically several meV) relevant for the reservoir-condensate coupling. The second-order diagram of the phonon scattering for G_1 shown in Fig. 5 yields again in the quasiparticle approximation for thermalized x and a thermal phonon bath with $n_{i,k} = \frac{1}{e^{\beta\hbar\omega_{i,k}}-1}$ for $i = \{a,\text{LO}\}$

$$\begin{aligned}\text{Re}R^{\text{x-c}}_{\text{i-ph}} &= \frac{2\pi}{\hbar}\sum_{\mathbf{k}} g^{\text{x-ph},2}_{i,k}\delta(\epsilon_k + E_0 - \hbar\omega_{i,k}) \\ &\quad\times [f_k(1+n_{i,k}) - (1+f_k)n_{i,k}] \\ &\simeq \frac{2\pi}{\hbar}\beta F g^{\text{x-ph},2}_{i,k'} N_x e^{-\beta(\hbar\omega_{i,k'}-E_0)}.\end{aligned} \tag{40}$$

Only the phonon emission processes are important, because the thermal population $n_{i,k}$ of the resonant phonons is very small. $\vec{k}' = \{k; x, k_y, \pi/L_z\}$ is the phonon wave number which fulfills the energy conservation

$$\epsilon_{k'} = \hbar\omega_{i,k'} - E_0. \tag{41}$$

In order to calculate again the corresponding complex scattering amplitude we have to evaluate the diagram $\Sigma_{\frac{1}{2},\text{i-ph}}(X,X')$ of Fig. 6 for the order parameter equation with two inner propagators G and the phonon propagator D. Taking, e.g., the contribution for the scattering from the reservoir to the condensate, i.e., $-\Sigma^{<}_{\frac{1}{2},\text{i-ph}}(X,X')$, we get by inserting again a still to be determined phase factor a_2 (omitting for conciseness again the central coordinates)

$$\begin{aligned}&-ia_2\sum\int d^2r\int_0^\infty dt\, g^{\text{x-ph},2}_{k_1,i} G^{<}(k_1,\omega_1)D^{>}(k_2,\omega_2) \\ &\times e^{i(k_1-k_2)\cdot r}e^{-i(\omega_1-\omega_2)t-\gamma t}\end{aligned} \tag{42}$$

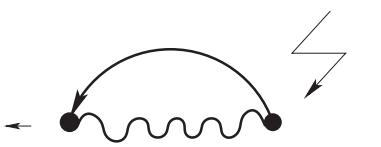

FIG. 6. Second-order x-phonon scattering self-energy $\Sigma^{\text{x-c}}_{\frac{1}{2}\text{x-ph}}$ for the GP equation.

and after the integration over r and t and using the Baym-Kadanoff ansatz

$$+ia_2\sum g_{k,i}^{\text{x-ph},2} f_k(1-n_{i,k})\frac{-1}{-i(e_k-\omega_k,i)-\gamma} = ia_2\sum \frac{g_{k,i}^{\text{x-ph},2} f_k(1+n_{i,k})}{i(e_k-\omega_{k,i})+\gamma} \quad (43)$$

or

$$ia_2\sum g_{k,i}^{\text{x-ph},2} f_k(1+n_{i,k})\left(\frac{\gamma-i(e_k-\omega_{i,k})}{(e_k-\omega_{i,k})^2+\gamma^2}\right). \quad (44)$$

With the choice $a_2=1$ we get the contribution to the nonequilibrium GP equation the result in the limit $\gamma\to 0$:

$$\frac{i\hbar}{2}\sum g_{k,i}^{\text{x-ph},2} f_k(1+n_{i,k})\left(\frac{\pi}{\hbar}\delta(e_k-\omega_{i,k})-i\frac{2}{\hbar}\frac{\text{P}}{e_k-\omega_{i,k}}\right). \quad (45)$$

The imaginary part of the phonon-assisted scattering amplitude is thus with the final replacement $e_k=E_0+\epsilon_k$ and the addition of the back-scattering contribution

$$\text{Im}R_{\text{i-ph}}^{\text{x-c}}=\frac{-2}{\hbar}\text{P}\sum_{\mathbf{k}} g_{i,k}^{\text{x-ph},2}\frac{f_k(1+n_{i,k})-(1+f_k)n_{i,k}}{\epsilon_k+E_0-\hbar\omega_{i,k}}. \quad (46)$$

Note that we had to choose the phase factor $a_3=i$ for the scattering diagram of Fig. 3 with 3 inner propagators, while we obtained here with 2 inner propagators $a_2=1$ to have consistent particle conservation. These choices can be unified in the following rule: The phase factor in the diagrams with N inner propagators has to be chosen as $a_N=i^{N-2}$.

The x-phonon interaction elements are given in the appendix for acoustic (a) and LO phonons. Obviously the rate has the linear dependence of the x concentration, as the phenomenologically assumed rates used so far. Note that there is no cross-section dependence of the resulting x-ph scattering rate because the $1/F$ from the square of the matrix element cancels against the area F in the rate expression (40). It will turn out that in particular the dispersive shifts due to the LO phonon transitions will have a physically important contribution in connection with the spontaneous structure formation discussed in Sec. V.

Naturally, higher order scattering processes like inelastic scattering and multiphonon scattering will additionally contribute to the scattering rates between the reservoir and the condensate.

IV. DISCUSSION OF THE RESULTING GP EQUATION

With the corresponding extensions the nonequilibrium GP equation is

$$\left(i\hbar\frac{\partial}{\partial T}+\frac{\hbar^2\nabla^2}{2m_c}-U(\mathbf{R},T)\right)\Psi(\mathbf{R},T) = g_0|\Psi(\mathbf{R},T)|^2\Psi(\mathbf{R},T) + \frac{i\hbar}{2}(R^{\text{x-c}}-2\gamma_c+i\text{Im}R^{\text{x-c}})\Psi(\mathbf{R},T), \quad (47)$$

where the total scattering amplitude is the sum of those for the p-p and the two phonon-assisted transitions:

$$R^{\text{x-c}}=R_{\text{p-p}}^{\text{x-c}}+\sum_{i=a,\text{LO}} R_{\text{i-ph}}^{\text{x-c}}. \quad (48)$$

For a reservoir in local thermal equilibrium described by the density N_x only (i.e., disregarding possible temperature variations) we display the above derived density dependence of the complex transition rates explicitly:

$$R^{\text{x-c}}=S_{\text{p-p}}^{\text{x-c}}N_x^2(\mathbf{R},T)+S_{\text{a-ph}}^{\text{x-c}}N_x(\mathbf{R},T)+S_{\text{LO-ph}}^{\text{x-c}}N_x(\mathbf{R},T). \quad (49)$$

In the nonequilibrium GP (47) and (32) we used for consistency the center coordinates $\mathbf{R},T$ for the spatial coordinate and time. The real part of the x-c coupling function describes the gain which is reduced by the cavity losses γ_c. Particle conservation $dN_x/dt=-d|\Psi(x)|^2/dt$ requires that the gain is $R^{\text{x-c}}/2$ for all three kinds of transitions as it has been found explicitly. The dispersive contributions of the included dissipative rates are given by the sum of the principal value integrals related to the rates (27) and (40). As mentioned, the gain (17) and the dispersive shift (18) due to p-p scattering from the reservoir to the condensate agree with the ones derived earlier by an equation of motion technique combined with an adiabatic elimination [14,20]. The shifts due to p-p, p-a-ph, and p-LO-ph scattering add to the blueshift of the condensate contained in $\mu\simeq g_0N_0$ with increasing pump power.

The nonequilibrium GP equation is still a homogeneous equation; thus if the order parameter was zero at an initial time it will stay so forever. Thus at least a dynamical symmetry breaking in the form of a small but finite initial value has to be included. A better choice is to assume stochastically distributed fluctuations as an initial value of $\Psi(\mathbf{R},T=0)$ [15]. Naturally if one wants to determine correlations of the order parameter the GP equation has to be extended by stochastic Langevin fluctuation fields which are connected with all dissipative processes as, e.g., treated by Wouters and Savona [11].

For the reservoir we will limit ourselves in the following to the rate equation for the x density. From Eq. (32) one gets by including also the x-phonon scattering rates the following reservoir rate equation:

$$\frac{\partial N_x}{\partial T}=P(\mathbf{R},T)-\text{Re}R^{\text{x-c}}(\mathbf{R},T)|\Psi(\mathbf{R},T)|^2-2\gamma_xN_x, \quad (50)$$

into which the total rate (49) due to x-c and x-i-ph scattering has to be inserted.

A pair of equations like (47) and (50) has been used recently [15] to explain the observed spontaneous structure formation with phenomenologically chosen x-c rate and shift. The pump beam had a ring structure, which in turn created a ring-shaped x-reservoir distribution $N_x(\mathbf{R},T)$ resulting finally in a ring-shaped polariton condensate $\Psi(\mathbf{R},T)$. In the corresponding simulations the x-c particle-particle scattering rate between the reservoir and the condensate has been taken as proportional to N_x as that obtained for the phonon scattering alone. More generally the scattering rate should be a sum of a linear and a quadratic term in N_x as derived above.

It is interesting that in the theory of BEC in atomic gases very similar concepts have been developed to describe the

condensate by a dissipative GP equation while the coexisting thermal cloud is described by a coupled quantum Boltzmann equation [21]. This theory is referred to as the ZNG approach according to the initials of the authors; for a recent review see Ref. [22].

BEC as a nonequilibrium second-order phase transition

The nonequilibrium GP equation (47) has a rather similar structure as the equation for a single laser mode after an adiabatic elimination of the polarization. Both equations are of first order in the time derivative and are driven by the difference of gain and loss. A derivation of the gain in analogy to the laser theory has been given in Ref. [20] for a single-mode BEC theory and refined in Ref. [14]. A stochastic extension of this formulation has been used for linewidth calculations. Naturally the difference between these single-mode theories and the nonequilibrium GP equation is that the spatial dependence of the order parameter field allows one to study a much richer scenario of spatial structures typical for quantum gases, while the nonlinear single-mode laser equation allows one to investigate only temporal structures. Only a laser theory formulated in terms of a nonlinear wave equation for the electric light field in the cavity would have a comparable richness of spatial-temporal phenomena.

In order to illuminate the close relation of the nonequilibrium BE theory and the laser theory we make use of the concept of the Ginzburg-Landau theory for nonequilibrium phase transitions. Quite generally, one can introduce the Ginzburg-Landau potential in the stochastic theory of the Fokker-Planck equation with a drift term and a diffusion term [24]. The drift term can be expressed in terms of a functional derivative of the Ginzburg-Landau potential and it appears again in the associated Langevin equation next to the fluctuations. In order to make contact with these concepts, we assume that the reservoir variable N_x can be eliminated, neglecting for the time being the temperature equation. N_x can be adiabatically eliminated, if $\gamma_x \gg \gamma_c$, which however for present-day microcavities is not the case. Note however that in an application of the reservoir-condensate equations for the description of spontaneous structure formation [15] it has been assumed (without further discussion) that $\hbar\gamma_x = 10$ meV $> \gamma_c = 1$ meV. Anyhow we describe the result of an adiabatic elimination of the reservoir for the purpose of illustration. For the reservoir density (32) we assume $dN_x/dt \ll 2\gamma_x N_x$. For the simpler case of a linear x density dependence of the x-c transition rate, i.e., $R^{\text{x-c}} = r^{\text{x-c}} N_x$, we obtain the adiabatic solution

$$N_x = \frac{P}{r^{\text{x-c}}|\Psi|^2 + 2\gamma_x} \simeq \frac{P}{2\gamma_x}\left(1 - \frac{r^{\text{x-c}}|\Psi|^2}{2\gamma_x}\right). \tag{51}$$

It should be noted that this stationary equation holds generally for stationary pumping. Separating the phase with $\Psi = e^{-i\phi}|\Psi|$ and inserting this ansatz and N_x into the nonequilibrium GP equation (47), one obtains the phase

$$\phi(t) = \int_0^t dt(\mu_c + \text{Im}r^{\text{x-c}} N_x) = \int_0^t dt(g_0|\Psi|^2 + \text{Im}r^{\text{x-c}} N_x) \tag{52}$$

and the equation of motion for $|\Psi|$

$$\frac{\partial|\Psi|}{\partial t} = -\frac{\delta V[|\Psi|]}{\delta|\Psi|} = \frac{1}{2}\left[\frac{r^{\text{x-c}}P}{2\gamma_x}\left(1 - \frac{r^{\text{x-c}}|\Psi|^2}{2\gamma_x}\right) - 2\gamma_c\right]|\Psi|, \tag{53}$$

where the functional $VV[|\Psi|]$ is the Ginzburg-Landau potential. The first term on the right-hand side of (54) is a functional derivative of $V[|\Psi|]$. A nonequilibrium GP equation of this type has been postulated—not derived—by Keeling and Berloff for MC polaritons [23]. The resulting Ginzburg-Landau potential is

$$V[|\Psi|] = \left(\frac{\gamma_c}{2} - \frac{r^{\text{x-c}}P}{4(2\gamma_x)}\right)|\Psi|^2 + \frac{r^{\text{x-c},2}P}{8(2\gamma_x)^2}|\Psi|^4. \tag{54}$$

This is the paradigmatic Ginzburg-Landau potential of a second-order nonequilibrium phase transition. Below the threshold pump power $P_{\text{th}} = 4\frac{\gamma_c}{\gamma_x r^{\text{x-c}}}$ the parabola $|\Psi|^2$ has a minimum at $|\Psi| = 0$. At threshold there is a critical slowing down; i.e., the parabola widens and becomes eventually negative. The positive fourth-order term together with the negative second-order parabola provides a new minimum at a finite $|\Psi|$ value. Stochastic forces will cause fluctuations of the order parameter around its minimum. If one plots the potential as a function of the polar coordinates ϕ and $|\Psi|$, one gets the well-known Mexican hat structure.

Next we turn to the treatment of realistic polariton microcavities in which the exciton lifetime on the order of ns is about 1 to 2 orders of magnitude longer than the photon lifetime in the cavity (order of several ps); i.e., $\gamma_x \ll \gamma_c$. Under this condition the dynamics of the x density slaves that of the condensate wave function; i.e., the condensate wave function follows nearly instantaneously the value of N_x. For the elimination of $N_x(t)$ one has to integrate the rate equation of N_x in time.

The nonequilibrium GP equation described by condensate-reservoir equations or by its simplified form obtained after elimination of the reservoir yield for the excitations a modified Bogoliubov spectrum as shown by Wouters and Carusotto [10] and Keeling and Berloff [23], respectively. The frequency spectrum of the nonequilibrium condensates goes to zero already at a finite k value and is purely imaginary below this point.

V. APPLICATION OF THE GP EQUATION FOR PATTERN FORMATION

Recently a series of papers used spatially structured, nonresonant excitation beams in the form of rings [15], a symmetrical array of several dots [25], and a central dot surrounded by one or several rings [26,27]. A series of interesting nonlinear dynamical effects have been seen, like spontaneous pattern formation, coexistence between localized and freely propagating condensates, and the spontaneous formation of vortex-antivortex pairs.

As an example for the use of the above derived nonequilibrium GP equation (47) and (50) with its microscopically determined rates and shifts we will calculate the pattern formation for CdTe microcavities. As in the experiment a bath temperature of 4 K is assumed, while the reservoir temperature is taken to be 20 K; i.e., the reservoir is not in equilibrium with

the lattice. The higher temperature increases the x-c transition rates. The depth of the photon-like part is taken as $E_0 = 13$ meV with a LO-phonon energy of $\hbar\omega_{\rm LO} = 21$ meV. The x Rydberg is $E_b = 25$ meV, and the x Bohr radius is $a_B = 5$ nm. For all other material parameters we refer, e.g., to Ref. [28]. For the real and imaginary part of the p-p scattering amplitude we use the analytical results (33) and (34) while the momentum integrals of the phonon-assisted scattering amplitudes are calculated numerically with a finite damping constant $\gamma = 2$ meV in the resonance denominator (40) and (46) [as, e.g., in the form of (44)]. We list the values used in the calculation by us and compare them by the values used by Manni *et al.* [15]: $\hbar g_o = 1.8 \times 10^{-3}/8,\ 2.4 \times 10^{-3}$ [15] meV μm^2, $\hbar\gamma_x = 10^{-2}, 10$ [15] meV, $\hbar\gamma_c = 0.1, 1.0$ [15] meV. In the subsection on BEC as a second-order nonequilibrium phase transition we commented already on the surprisingly large reservoir damping constant used by Manni *et al.* The damping constants chosen by us correspond to an exciton lifetime $\tau_x = 120$ ps and to a cavity lifetime $\tau_c = 6$ ps. The values of the resulting rates and shifts (50) due to the interaction with longitudinal optical phonons are $\hbar{\rm Re}S^{\rm x\text{-}c}_{\rm LO\text{-}ph} = 1.0 \times 10^{-4}$ meV μm^2, $\hbar{\rm Im}S^{\rm x\text{-}c}_{\rm LO\text{-}ph} = -1.7 \times 10^{-4}$ meV μm^2. The corresponding results for acoustic phonon scattering are $\hbar{\rm Re}S^{\rm x\text{-}c}_{\rm a\text{-}ph} = 1.0 \times 10^{-3}, 10^{-1}$ [15] meV μm^2, $\hbar{\rm Im}S^{\rm x\text{-}c}_{\rm a\text{-}ph} = -1.5 \times 10^{-3},\ -2.2 \times 10^{-2}$ [15] meV μm^2. Finally the quadratic particle-particle scattering rates are $\hbar{\rm Re}S^{\rm x\text{-}c}_{\rm p\text{-}p} = 4.7 \times 10^{-7}$ meV μm^4, $\hbar{\rm Im}S^{\rm x\text{-}c}_{\rm p\text{-}p} = -1.2 \times 10^{-6}$ meV μm^4. Such quadratic processes in N_x have not been included in the simulations of Manni *et al.* Their phenomenologically chosen transition amplitudes linear in N_x are of a similar size as our calculated rates and shifts for the acoustic-phonon assisted processes alone.

We will demonstrate that the nonequilibrium GP equations with a microscopically calculated scattering amplitude which is the sum of linear and quadratic terms in the exciton density N_x are able to reproduce at least qualitatively the observed spontaneous pattern formation. Furthermore, we highlight the importance of the nonlinear frequency shifts not only due to the third-order term in the GP equation but also due to those depending on the exciton density N_x for the occurrence of pattern formation. This can be seen most directly, if one assumes N_x is expressed in terms of Ψ and eliminated, as shown above; these shifts become nonlinear in Ψ too.

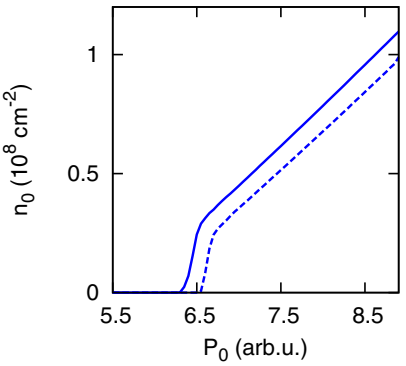

FIG. 7. (Color online) Mean condensate density versus pump power for the combined p-p and p-phon coupling (full line) and the p-phon coupling alone (dashed line) versus pump power.

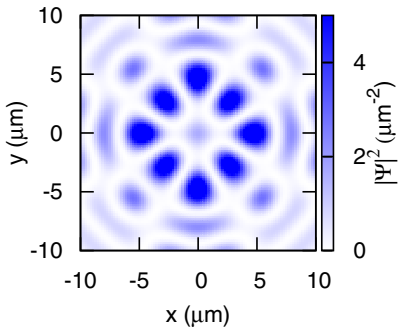

FIG. 8. (Color online) Plot of the amplitude of the polariton condensate.

We use the nonequilibrium GP (47) for CdTe MC polaritons with a spatially structured pump rate of the form

$$P(\mathbf{R},T) = p_0 \tanh\left(\frac{T}{t_0}\right) \exp\left(-\frac{\sqrt{x^2+(\epsilon y)^2}-(\epsilon r_0)^2}{w^2}\right), \tag{55}$$

where $r_0 \neq 0$ for ring excitation and $\epsilon = 1$ for excitation profiles with circular symmetry. For the numerical solution of the nonequilibrium GP equation we use a split step Fourier transform method. As initial conditions we assume an empty reservoir and an infinitesimally small order parameter with a white noise fluctuating amplitude and phase. The switching-on time is taken to be $t_0 = 10^{-2}$ ps with a radius $r_0 = 5$ μm for ring excitations and the width is $w_0 = 0.34$ μm similar as in the experiments [15]. Separating again phase and amplitude of the condensate wave function $\psi = |\psi|e^{i\phi}$, we find as shown in Fig. 7 for ring excitation the mean condensation density for the combined p-p and p-phon coupling (full line) and the p-phon coupling alone (dashed line) versus pump power. It is seen that the quadratic p-p scattering between the reservoir and condensate lowers the threshold and increases the condensate density substantially, although it alone is not sufficient to reach condensation. Next we present in Fig. 8 the spontaneous structure formation in which the condensate on the ring breaks up into an eightfold lobe structure. Similar structures have been found both in the experiment and the simulation by Manni *et al.* [15]. The corresponding plot of the phase varying from $-\pi$ to $+\pi$ is shown in Fig. 9.

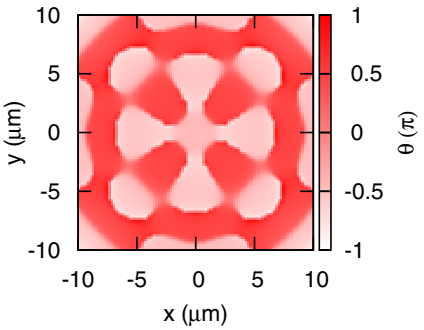

FIG. 9. (Color online) Plot of the phase of the polariton condensate.

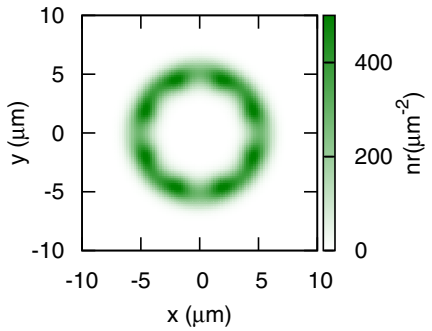

FIG. 10. (Color online) Plot of the reservoir exciton density.

Finally, Fig. 10 shows for reservoir exciton density only a weak modulation due to the back action of the structured condensate. The dynamics of the condensation is shown in Fig. 11 where the condensate density and the reservoir density are plotted versus time. One sees an initial overshoot of the reservoir density over its stationary value which is reached after the condensation is established again with an overshoot and some relaxation oscillations. The delay between the formation of the populations of the reservoir and of the condensate is in the experiment much smaller than the calculated delay of 1 ns. Here the relatively inaccurate description of the reservoir in the initial time period during and immediately after the switching-on of the laser excitation shows up. In this period the description in terms of only x bosons which are furthermore assumed to be in a thermal equilibrium is too simple a picture. Another reason for the delayed condensate formation is the fact that we did not give a full stochastic description with Langevin fluctuation, but include noise only in the initial condition. Mainly to avoid a retarded condensation the concept of a second reservoir of inactive excitons was introduced [18]. Whether the above derived temperature rate equation can also be important in this respect has to be left to later investigations.

For the pattern formation a sufficiently large value of the nonlinear shifts $\mathrm{Im}S^{\text{x-c}}_{\text{p-p}}N_x^2 + \sum_{i=a,\text{LO}} \mathrm{Im}S^{\text{x-c}}_{\text{i-ph}}N_x$ is of crucial importance. One may wonder why a shift proportional to N_x contributes to structure formation based on a nonlinear GP equation. However, one should keep in mind that if N_x is eliminated in the GP equation, a nonlinearity in $|\psi|$ results, as discussed above. By numerical variation

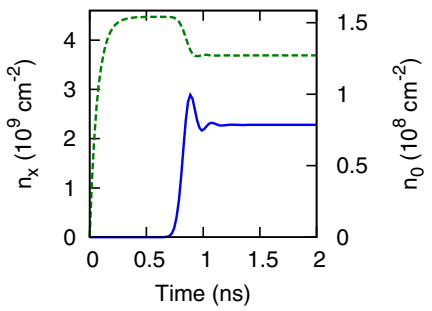

FIG. 11. (Color online) Plot of the reservoir exciton density (dashed green line) and the condensate density (full blue line) versus time.

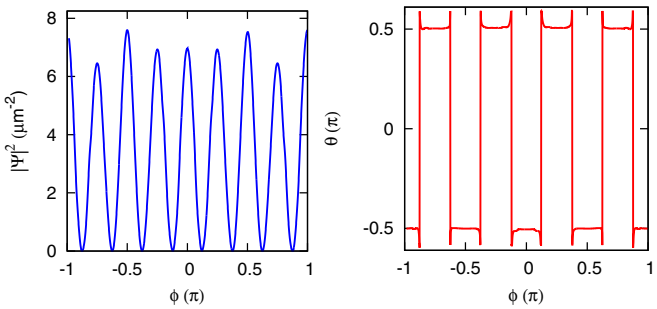

FIG. 12. (Color online) Plots of amplitude (left, blue) and phase here called Θ (right, red) versus the rotational angle ϕ at a radius of 4.5 μm at which the amplitude peaks occur in Fig. 8.

we found that for structure formation the dispersive shifts had to be larger than $\hbar|\mathrm{Im}S^{\text{x-c}}_{\text{p-p}}| \geqslant 0.8 \times 10^{-6}$ meV μm^4 and $\hbar|\mathrm{Im}S^{\text{x-c}}_{\text{a-ph}}| \geqslant 0.9$ meV μm^2. The crucial role of the phase in pattern formation can also be seen from a plot of amplitude and phase versus the angle ϕ at a radius at which the amplitude peaks occur in Fig. 8 (see Fig. 12).

While the condensate density varies relatively smoothly, the phase shows sharp changes with spikes at the end of the phase walls as is typical for solitary structures.

In conclusion we have derived by quantum kinetic techniques the nonequilibrium Gross-Pitaevskii equations for condensed exciton polaritons in microcavities. As originally proposed by Wouters and Carusotto [10] we get a nonlinear Schrödinger equation with gain and loss terms and a quantum Boltzmann equation for the excitons in the reservoir which feeds the condensate by phonon-assisted and by particle-particle scattering processes. The transition rates and the corresponding shifts are evaluated explicitly for the mentioned gain processes. Particularly the excitonic gain due to particle-particle scattering is quadratic in the reservoir exciton density which so far has been overlooked. We show how one can formulate for reservoirs in local thermal equilibrium not only a rate equation but also an equation for the time and space dependent temperature of the reservoir. Simple analytic expressions for the x-c scattering rate and the corresponding shift are derived. We discuss under which conditions the reservoir can be eliminated adiabatically in order to obtain a Ginzburg-Landau potential for a nonequilibrium second-order phase transition. Finally we apply our microscopic model to illustrate that it can describe at least qualitatively the spontaneous pattern formation observed and simulated phenomenologically by Manni *et al.* [15].

ACKNOWLEDGMENTS

This work has been supported by the Research Networking Programme POLATOM of the European Science Foundation. T. D. Doan gratefully acknowledges the financial support of the National Foundation for Science and Technology Development (NAFOSTED). Stimulating discussions with Jonathan Keeling, Nick Proukakis, Benoit Deveaud, and Laci Banyai are acknowledged.

APPENDIX: PHONON SCATTERING

The frequency of acoustic (a) phonons $\omega_{a,k} = c_s k$ with $k = \sqrt{k_{||}^2 + (\pi/L_z)^2}$, where L_z is the quantum well thickness and c_s is the sound velocity. The interaction matrix elements are in the long-wavelength limit given by

$$g_{a,q}^{\text{x-ph}} = [G_e L_e(q) - G_h L_h(q)] \sqrt{\frac{\hbar q}{2\rho F L_z c_s}}. \tag{A1}$$

Here, G_e and G_h are the electron and hole deformation potentials, respectively. ρ and c_s are the density and longitudinal sound velocity. L_z is the quantum well thickness. The superposition integrals of the x wave functions and the phonon plane wave

$$L_i(q) = \left[1 + \left(\frac{m_i q a_0}{2(m_e + m_h)}\right)^2\right]^{-\frac{3}{2}}. \tag{A2}$$

Similarly the interaction with LO phonons $\omega_{\text{LO},k} = \omega_0$ is given by the matrix element of the Fröhlich coupling

$$g_{\text{LO},q}^{\text{x-ph}} = [L_e(q) + L_h(q)] \frac{e}{q} \sqrt{\frac{\hbar\omega_0}{F L_z} \left(\frac{1}{\epsilon_\infty} - \frac{1}{\epsilon_0}\right)}. \tag{A3}$$

ϵ_∞ and ϵ_0 are the high-frequency and static dielectric constants.

Next we discuss briefly the inter-reservoir scattering of the excitons with acoustic phonons. The scattering rate is for a nondegenerate x gas for emission and absorption of an acoustic phonon:

$$r_k^a = -\frac{2\pi}{\hbar} \sum_{\mathbf{q},\pm\mathbf{1}} g_{a,q}^{\text{x-ph},2} (f_k - f_{k-q}) \delta(\epsilon_k - \epsilon_{k-q} \mp \hbar\omega_{a,q}) \times \left(n_{a,q} + \frac{1}{2} \pm \frac{1}{2}\right). \tag{A4}$$

Assuming a small deviation from the equilibrium distribution with bath temperature f_k^0, we put $f_k = \delta f_k + f_k^0$ and get with detailed balance in equilibrium the relaxation time approximation

$$r_k^a \simeq \frac{f_k^0 - f_k}{\tau_k^a} \quad \text{with} \quad \frac{1}{\tau_k^a} = \frac{2\pi}{\hbar} \sum_{\mathbf{q},\pm\mathbf{1}} g_{a,q}^{\text{x-ph},2} \times \delta(\epsilon_k - \epsilon_{k-q} \mp \hbar\omega_{a,q}) \left(n_{a,q} + \frac{1}{2} \pm \frac{1}{2}\right). \tag{A5}$$

Note that the particle conservation requires a k-independent relaxation time, so that $1/\tau_k^a$ has to be averaged over k in the relevant momentum region:

$$\frac{1}{\tau^a} \simeq \frac{1}{N_x} \frac{1}{F} \sum_{\mathbf{k}} \frac{f_k^0}{\tau_k^a}. \tag{A6}$$

[1] M. H. Anderson, J. R. Elesin, M. R. Matthews, C. E. Wiemann, and E. A. Cornell, Science **269**, 198 (1995).
[2] K. B. Davis, M. O. Mewes, M. R. Andrews, N. J. van Druten, D. S. Durfee, D. M. Kurn, and W. Ketterle, Phys. Rev. Lett. **75**, 3969 (1995).
[3] C. C. Bradley, C. A. Sackett, J. J. Tollett, and R. G. Hulet, Phys. Rev. Lett. **75**, 1687 (1995).
[4] S. O. Demokritov *et al.*, Nature (London) **443**, 430 (2006).
[5] H. Deng, G. Weihs, D. Snoke, J. Bloch, and Y. Yamamoto, Proc. Natl. Acad. Sci. USA **100**, 15318 (2003); H. Deng, H. Haug, and Y. Yamamoto, Rev. Mod. Phys. **82**, 1489 (2010).
[6] J. Kasprazk, M. Richard, S. Kundermann, A. Baas, P. Jeanbrun, J. M. J. Keeling, F. M. Marchetti, M. H. Symanska, R. Andre, J. L. Staehli, V. Savona, P. B. Littlewood, B. Deveaud-Pledran, and Le Si Dang, Nature (London) **443**, 409 (2010).
[7] E. P. Gross, Il Nuovo Cimento **20**, 454 (1961).
[8] L. P. Pitaevskii, Sov. Phys. JETP **13**, 451 (1961).
[9] I. A. Shelykh, Y. G. Rubo, G. Malpuech, D. D. Solnyshkov, and A. Kavokin, Phys. Rev. Lett. **97**, 066402 (2006).
[10] M. Wouters and I. Carusotto, Phys. Rev. Lett. **99**, 140402 (2007).
[11] M. Wouters and V. Savona, Phys. Rev. B **79**, 165302 (2009).
[12] L. P. Kadanoff and G. Baym, *Quantum Statistical Mechanics* (W. A. Benjamin, New York, 1962).
[13] H. Haug and A. P. Jauho, *Quantum Kinetics in Transport and Optics of Semiconductors* (Springer, Berlin, 1996).
[14] H. Haug, T. D. Doan, H. T. Cao, and D. B. Tran Thoai, Phys. Rev. B **85**, 205310 (2012).
[15] F. Manni, K. G. Lagoudakis, T. C. H. Liew, R. Andre, and B. Deveaud-Pledran, Phys. Rev. Lett. **107**, 106401 (2011).
[16] H. Haug and S. W. Koch, *Quantum Theory of the Optical and Electronic Properties of Semiconductors* (Springer, Berlin, 2009).
[17] B. Deveaud-Pledran (private communication).
[18] K. G. Lagoudakis, F. Manni, B. Pietka, M. Wouters, T. C. H. Liew, V. Savona, A. V. Kavokin, R. Andre, and B. Deveaud-Pledran, Phys. Rev. Lett. **106**, 115301 (2011).
[19] M. Assmann, J.-S. Tempel, F. Veit, M. Bauer, A. Rahimi-Iman, A. Löfler, S. Höfling, S. Reitzenstein, L. Worschech, and A. Forchel, Proc. Natl. Acad. Sci. USA **108**, 1804 (2011).
[20] H. Haug, H. T. Cao, and D. B. Tran Thoai, Phys. Rev. B **81**, 245309 (2010).
[21] E. Zaremba, T. Nikuni, and A. Griffin, J. Low Temp. Phys. **116**, 277 (1999).
[22] N. P. Proukakis and B. Jackson, J. Phys. B: At., Mol. Opt. Phys. **41**, 203002 (2008).
[23] J. Keeling and N. G. Berloff, Phys. Lett. **100**, 250401 (2008).
[24] R. Graham and H. Haken, Z. Physik **237**, 31 (1970).
[25] P. Cristofolini, A. Dreismann, G. Christmann, G. Franchetti, N. G. Berloff, P. Tsotsis, Z. Hatzopoulos, P. G. Savvidis, and J. J. Baumberg, Phys. Rev. Lett. **110**, 186403 (2013).
[26] G. Roumpos, M. D. Fraser, A. Löffler, S. Höfling, A. Forchel, and Y. Yamamoto, Nat. Phys. **7**, 129 (2011).
[27] F. Manni, T. C. H. Liew, K. G. Lagoudakis, C. Ouellet-Plamondon, R. Andre, V. Savona, and B. Deveaud, Phys. Rev. B **88**, 201303 (2013).
[28] T. D. Doan, H. T. Cao, D. B. Tran Thoai, and H. Haug, Phys. Rev. B **74**, 115316 (2006).